Application Note 29

Prism Compressor for Ultrashort Laser Pulses

Technology and Applications Center

The Effect of Dispersion on Ultrashort Pulses

In the time domain, the electric field for a Gaussian pulse with a carrier frequency, ω_0, pulse duration, Δt, and phase, $\theta(t)$, can be described by,

$$E(t) = \sqrt{A_t e^{-\ln 2\left(\frac{2t}{\Delta t}\right)^2}}\, e^{-i(\omega_0 t + \theta(t))} + c.c. \qquad (1)$$

where c.c. denotes the complex conjugate. In this expression, A_t is the amplitude of the pulse, ω_0 determines the color of the pulse, Δt determines the minimum pulse duration and consequently the bandwidth of the pulse, and $\theta(t)$ determines the temporal relationship among the frequency components contained within the bandwidth of the pulse. $\theta(t)$ plays an important role in altering the pulse duration. It is the term that is responsible for pulse broadening in dispersive media and can be thought of as adding a complex width to the Gaussian envelope.

The description of the Gaussian pulse given by (1) is intuitive in the sense that it is fairly straightforward to conceptualize a pulse in the time domain. However, when dealing with pulses traveling through dispersive media, it can be problematic to work in the time domain. For example, in order to determine the duration of a pulse after traveling through some dispersive material, it is necessary to solve a convolution integral[1] which in general must be done numerically. However, due to the fact that convolutions become products upon a Fourier transformation[2], it is convenient to solve this type of problem in the frequency domain.

Time and frequency along with position and momentum represent a class of variables known as Fourier pairs.[2] Fourier pairs are quantities that can be interconnected through the Fourier transform. Performing a Fourier transform on equation (1) yields,

$$E(\omega) = \sqrt{A_\omega e^{-\ln 2\left(\frac{2(\omega-\omega_o)}{\Delta\omega}\right)^2}}\, e^{-i\varphi_{Pulse}(\omega-\omega_0)} \qquad (2)$$

(for the sake of brevity, negative frequency components are omitted). The electric field is now expressed as a function of frequency, $\Delta\omega$ and Δt are related through the uncertainty relation[1], $\Delta\omega\Delta t = 4\ln(2)$, and the spectral phase, $\varphi(\omega)$, describes the relationship between the frequency components of the pulse. In equation (2), ω as well as $\Delta\omega$ represent angular frequencies. Angular frequency can be converted to linear frequency, ν (i.e. the observable quantity), by dividing it by 2π, $\nu = \frac{\omega}{2\pi}$. In terms of the linear frequency, the uncertainty principle is given by, $c_B = \Delta\nu\Delta t = \frac{2\ln(2)}{\pi}$. When an input pulse, $E_{in}(\omega)$, passes through a dispersive medium, the phase added by the material is given simply by the product of the input field with the transfer function of the material. The emerging pulse $E_{out}(\omega)$, is given by,

$$E_{out}(\omega) = E_{in}(\omega)R(\omega)e^{-i\varphi_{Mat}(\omega-\omega_0)} \qquad (3)$$

where $\varphi_{Mat}(\omega-\omega_0)$ is the spectral phase added by the material and $R(\omega)$ is an amplitude scaling factor which for a linear transparent medium can be approximated by, $R(\omega) \approx 1$.[1]

It is a common convention to express spectral phase as a Taylor expansion around the carrier frequency of the pulse as shown below,

$$\varphi(\omega-\omega_0) = \varphi_0 + \varphi_1\cdot(\omega-\omega_0) + \varphi_2\cdot\frac{(\omega-\omega_0)^2}{2} + \varphi_3\cdot\frac{(\omega-\omega_0)^3}{6} + \ldots \qquad (4)$$

This approach allows a more straightforward understanding of the effect of material dispersion on properties of the pulse. Taking into account that $\varphi(\omega) = k(\omega)L$, where k is the propagation constant, and L is the length of the medium, while also considering that the group velocity is defined as $\upsilon_G = d\omega / dk$, it is easy to see that first term in (4) adds a constant to the phase. The second term, proportional to $1/\upsilon_G$, adds delay to the pulse. Neither of these terms affects the shape of the pulse. The third term, referred to as group delay dispersion (GDD), is proportional to $\frac{d}{d\omega}\left(\frac{1}{\upsilon_G}\right)$, also known as group velocity dispersion (GVD). It introduces a frequency dependent delay of the different spectral components of the pulse, thus temporally changing it. The GDD and GVD are related through $\varphi_2(\omega) = k_2(\omega)L$. The fourth term, referred to as Third Order Dispersion (TOD) applies quadratic phase across the pulse. For the purpose of this note, we will truncate the series at the third term, GDD, only making references to higher order terms when necessary. Truncating equation (4) at the third term allows us to rewrite equation (3) for a Gaussian pulse as,

$$E_{out}(\omega) = \sqrt{A_\omega e^{-\ln 2\left(\frac{2(\omega-\omega_o)}{\Delta\omega}\right)^2}}\, e^{-i(\varphi_{2,Pulse}+\varphi_{2,Mat})\frac{(\omega-\omega_0)^2}{2}} \qquad (5)$$

hence phases in the frequency domain are simply additive. This result underscores the advantage of performing these types of calculations in the frequency domain.

To arrive at the new pulse duration, it is necessary to transform the spectral envelope of equation (5) back into the time domain. Performing this Fourier transform, the pulse envelope is given by,

$$E_{out}(t) = \sqrt{A_t'}\, e^{\frac{4(\ln 2)t^2}{2[\Delta t^2 + i4(\ln 2)\varphi_2]}} \qquad (6)$$

where φ_2 is the sum of the group delay dispersion of the material and the group delay of the pulse. In order to get the new pulse duration, Δt_{out}, it is necessary to obtain the intensity, $I_{out}(t)$, by squaring the electric field in equation (6) and then relating $I_{out}(t)$ to the general form for a Gaussian pulse,

$$e^{-\ln 2\left(\frac{2t}{\Delta t_{out}}\right)^2} = e^{\frac{4(\ln 2)t^2\Delta t^2}{\Delta t^4 + 16(\ln 2)^2\varphi_2{}^2}} \qquad (7)$$

Solving equation (7) for Δt_{out},

$$\Delta t_{out} = \frac{\sqrt{\Delta t^4 + 16(\ln 2)^2\varphi_2{}^2}}{\Delta t} \qquad (8)$$

provides an expression for the pulse duration. Finally, by solving equation (8) for group delay dispersion while replacing the transform limited pulse duration with the spectral bandwidth of the pulse, GDD can be expressed completely in terms of observables (i.e. pulse width and spectrum),

$$\varphi_2 = \frac{1}{4(\ln 2)}\sqrt{\left(\frac{c_B\Delta t_{out}}{\Delta\nu}\right)^2 - \left(\frac{c_B}{\Delta\nu}\right)^4} \qquad (9)$$

where $\Delta\nu = c\Delta\lambda/\lambda^2$. In general, c_B is a function of the pulse profile as shown in Table 1. It should be noted that equation (9) is strictly valid for Gaussian pulses.

Table 1. Time-bandwidth product C_B for various pulse profiles

Field Profile	Gaussian	Sech	Lorentzian
c_B	0.441	0.315	0.142

Dispersion in materials is defined by the group velocity dispersion. In order to estimate amount of GDD introduced by a material of length L, one has to calculate the wavelength dependent index of refraction, n(λ), typically in the form of a Sellmeier's type equation, and then calculate second derivative at the wavelength of interest.

GVD is related to the second derivative of refractive index with respect to wavelength by $GVD = \frac{\lambda^3}{2\pi c^2}\left(\frac{d^2 n}{d\lambda^2}\right)$. GDD is simply a product of GVD with the length of the material. The dispersive properties of several optical materials are shown in Table 2.

Table 2. Material parameters for fused silica, N-LakL21, N-SF10 and N-BK7 glass

Material	λ (nm)	n (λ)	dn/d λ (μm^{-1})	d^{2}n/d λ^2 (μm^{-2})	d^{3}n/d λ^3 (μm^{-3})	GVD (fs^2/mm)	TOD (fs^3/mm)
Fused Silica	400	1.4701	-0.1091	0.8609	-9.5997	97.43	30.2
	450	1.4656	-0.0758	0.5115	-4.9839	82.43	27.24
	500	1.4623	-0.0554	0.323	-2.8089	71.4	25.53
	550	1.4599	-0.0422	0.2135	-1.686	62.82	24.62
	600	1.458	-0.0333	0.1462	-1.0639	55.85	24.28
	650	1.4565	-0.0272	0.1029	-0.6993	49.98	24.42
	700	1.4553	-0.0228	0.074	-0.4755	44.87	24.99
	750	1.4542	-0.0196	0.054	-0.3328	40.3	25.99
	800	1.4533	-0.0173	0.0399	-0.2388	36.11	27.44
	850	1.4525	-0.0156	0.0296	-0.1751	32.18	29.36

Material	λ (nm)	n (λ)	dn/d λ (μm^{-1})	d^{2}n/d λ^2 (μm^{-2})	d^{3}n/d λ^3 (μm^{-3})	GVD (fs^2/mm)	TOD (fs^3/mm)
N-LAKL21	400	1.6593	-0.1793	1.4695	-16.9451	166.31	56.91
	450	1.6518	-0.1228	0.8604	-8.575	138.65	49.14
	500	1.6466	-0.0886	0.5387	-4.7519	119.08	44.56
	550	1.6428	-0.0667	0.3545	-2.8188	104.31	41.79
	600	1.6398	-0.052	0.2425	-1.7634	92.62	40.2
	650	1.6375	-0.0418	0.1709	-1.1515	83	39.49
	700	1.6356	-0.0345	0.1234	-0.7791	74.83	39.48
	750	1.634	-0.0292	0.0907	-0.5431	67.7	40.1
	800	1.6327	-0.0252	0.0677	-0.3884	61.32	41.33
	850	1.6315	-0.0223	0.0511	-0.284	55.47	43.18

Material	λ (nm)	n (λ)	dn/d λ (μm^{-1})	d^{2}n/d λ^2 (μm^{-2})	d^{3}n/d λ^3 (μm^{-3})	GVD (fs^2/mm)	TOD (fs^3/mm)
N-SF10	400	1.7783	-0.5472	6.0995	-102.657	690.32	546.73
	450	1.7569	-0.3345	2.9304	-37.7789	472.22	315.81
	500	1.7432	-0.2245	1.6362	-17.3375	361.69	220.47
	550	1.7337	-0.1603	1.0027	-9.1104	295.01	171.92
	600	1.7267	-0.1196	0.6548	-5.2463	250.13	143.87
	650	1.7215	-0.0925	0.448	-3.2284	217.58	126.33
	700	1.7174	-0.0736	0.3176	-2.0898	192.65	114.87
	750	1.714	-0.06	0.2316	-1.408	172.75	107.26
	800	1.7113	-0.05	0.1726	-0.9802	156.31	102.31
	850	1.709	-0.0424	0.1311	-0.7012	142.35	99.32

Material	λ (nm)	n (λ)	dn/d λ (μm^{-1})	d^{2}n/d λ^2 (μm^{-2})	d^{3}n/d λ^3 (μm^{-3})	GVD (fs^2/mm)	TOD (fs^3/mm)
N-BK7	400	1.5308	-0.1332	1.0768	-12.3136	121.87	40.71
	450	1.5253	-0.0917	0.6329	-6.2713	101.98	35.53
	500	1.5214	-0.0665	0.397	-3.4914	87.77	32.52
	550	1.5185	-0.0503	0.2615	-2.0782	76.94	30.78
	600	1.5163	-0.0395	0.1788	-1.3036	68.29	29.89
	650	1.5145	-0.0319	0.1258	-0.853	61.11	29.64
	700	1.5131	-0.0266	0.0906	-0.5781	54.95	29.93
	750	1.5118	-0.0227	0.0664	-0.4035	49.51	30.73
	800	1.5108	-0.0198	0.0492	-0.2889	44.59	32.03
	850	1.5098	-0.0177	0.0369	-0.2114	40.03	33.86

By measuring the spectrum and autocorrelation for a Gaussian pulse, equation (9) can be used to determine the amount of GDD. Figure 1 illustrates the results of a numerical simulation of the electric field for three pulses, all containing 100 nanometers of bandwidth, centered around 800 nanometers. The black curve corresponds to a pulse with the GDD set to zero, the red curve corresponds to a pulse with the GDD set to 500 fs^2 and the blue curve corresponds to a pulse with the GDD set to -500 fs^2. The pulse with the minimum time duration corresponds to the pulse having zero GDD. For the red pulse (positive chirp), the higher frequency components are lagging behind the lower ones and for the blue pulse (negative chirp), the lower frequency components are lagging behind the higher ones.

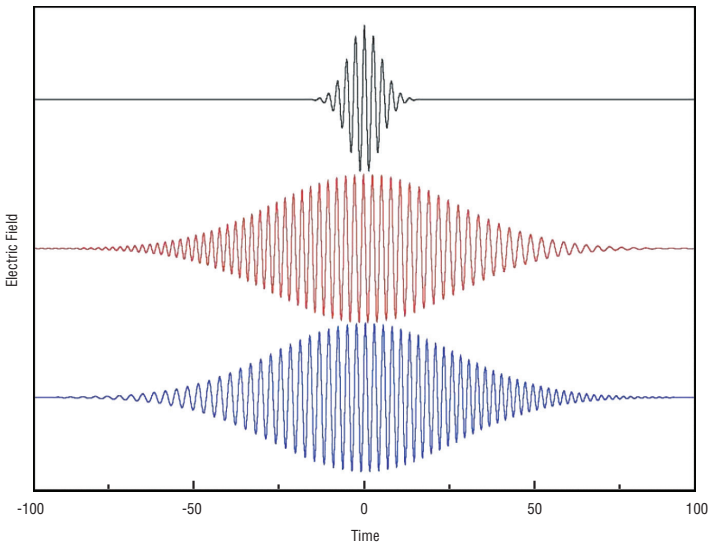

Figure 1. The effect of GDD on pulse with 100 nm bandwidth

Figure 2 shows the width of a Gaussian pulse at 800 nm before and after propagation through 20 mm of BK7 glass calculated using equation (8) and data from Table 2.

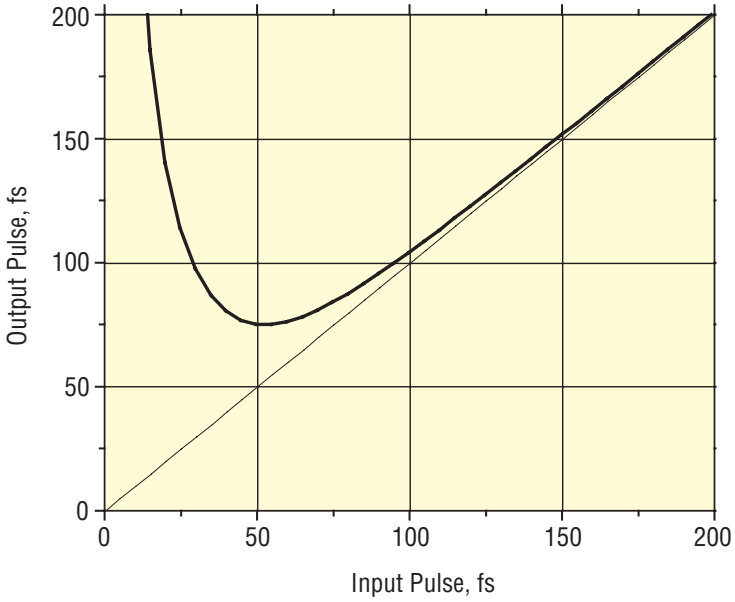

Figure 2. Broadening of a femtosecond pulse at 800 nm after propagation through 20 mm of BK7

The amount of introduced GDD in this case is about 1000 fs^2, and is equivalent to propagating the beam through only a few optical components. It is clear that the effect is not significant for pulses longer than 100 fs. However, a 25 fs pulse broadens by a factor of 4.

Dispersion Compensation Using a Prism Compressor

How can we compensate for the chirp acquired by a femtosecond pulse after propagation through a dispersive material? Angular dispersion produces negative GDD which may be introduced either through a sequence of prisms or gratings.[1,3,4,5] This note describes a simple and cost effective prism compressor suitable for compensation of GDD typical for common femtosecond setups based on oscillators, amplifiers and OPAs.

The unfolded geometry of the prism compressor consists of a four prism sequence as shown in Figure 3. The apex angle of each prism is equal to Brewster angle for a given wavelength and the prisms are arranged in such a way that the beam enters and exits each prism under Brewster angle. The reflection losses in that case are minimized for the P polarization. The first prism disperses the beam.

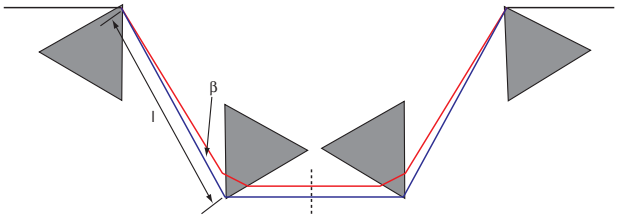

Figure 3. Geometrical arrangement of a four prism sequence for introducing negative GDD

The second prism collimates the dispersed beam. The third and fourth prisms undo the action of the first two such that the beams entering and exiting the compressor are spatially identical. The dashed line in Figure 3 represents a folding mirror which can be placed after the second prism and utilize two prisms instead of four in double pass geometry. It can be shown that a wavelength dependent path length, P(λ), due to dispersion is given by,

$$P = 2l\cos\beta \qquad (10)$$

where l is the distance between apex 1 and apex 2 of the first two prisms and β is the angle of the dispersed beam after the first prism.[4] The GDD introduced by the prism sequence is given by,

$$GDD_{PRISM} = \left(\frac{\lambda^3}{2\pi c^2}\right)\frac{d^2P(\lambda)}{d\lambda^2} \quad (11)$$

where λ is the wavelength of light and c is the speed of light. Utilizing the approach of Fork et al[4]., equation (11) can be written as,

$$GDD_{PRISM} = \frac{\lambda^3}{2\pi c^2}\left[4l\left\{\left[\frac{d^2n}{d\lambda^2} + \left(2n - \frac{1}{n^3}\right)\left(\frac{dn}{d\lambda}\right)^2\right]\sin\beta - 2\left(\frac{dn}{d\lambda}\right)^2\cos\beta\right\} + 4\left(\frac{d^2n}{d\lambda^2}\right)\left(2D_{1/e^2}\right)\right] \quad (12)$$

where n is the refractive index and $D_{1/e}$ is the beam diameter at $1/e^2$. The refractive index as well as the derivatives of the refractive index can be readily obtained from Sellmeier's equations for a given material (see Table 2) and β can be estimated from,

$$\beta \approx -2\frac{dn}{d\lambda}\Delta\lambda \quad (13)$$

Since β is relatively small and sin(β)<<cos(β) one can simplify Eq.(12) as,

$$GDD_{PRISM} \approx \frac{\lambda^3}{2\pi c^2}\left[-4l\left\{2\left(\frac{dn}{d\lambda}\right)^2\right\} + 4\left(\frac{d^2n}{d\lambda^2}\right)\left(2D_{1/e^2}\right)\right] \quad (14)$$

The first term is always negative and depends on prism separation. The second term is always positive and depends on the pathlength through the prisms. Varying the prism separation and the pathlength through the prisms one can control the sign and the amount of introduced dispersion. It should be noted, however, that at 800 nm for SF10 glass prisms, the sin(β) term in (12) introduces a 20% correction factor to the GDD for 50 nanometers of bandwidth. For that reason all calculations in this note were performed using the exact equation (12).

Building the Compressor

The experimental setup for the pulse compression is shown in Figure. 4. The compressor can be set up as follows:

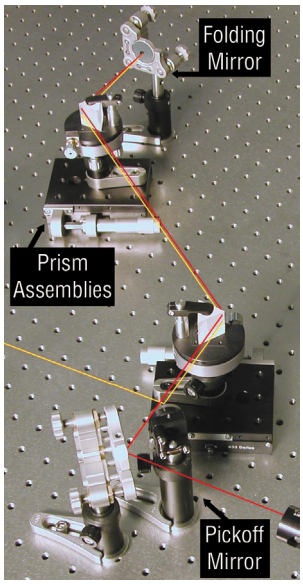

Figure 4. Experimental setup of the two-prism compressor

1 Determine the GDD responsible for elongating the pulse. This can be accomplished by measuring the spectrum and autocorrelation width, and then calculating the GDD from equation (9).

2. Determine the transform limited pulse duration Δt corresponding to the measured bandwidth from $\Delta t = \frac{c_B\lambda^2}{c\Delta\lambda}$. At 800 nm this expression simplifies to $\Delta t(fs) \approx \frac{940}{\Delta\lambda(nm)}$. This in conjunction with wavelength will be the primary determinants of the prism material. As a rule of thumb, SF10 can be used for pulse durations greater than 50 fs as long as the wavelength is above 400 nm. LakL21 can be used for pulses greater than 25 fs at wavelengths longer than 380 nm. Fused silica should be reserved for pulses shorter than 25 fs and wavelengths shorter than 380 nm.

3. Use data from Table 2 (first and second derivatives of refractive index) and solve equation (12) to determine the prism separation necessary to balance the positive GDD on the pulse for a given wavelength. Tables of prism distances for certain wavelengths are provided in Appendix 1, along with a guide explaining the proper use of these tables.
4. Assemble the Prism Assemblies as shown in Figure 5.
5. Prior to inserting the Prism 1 Assembly in the beam path, take care to ensure that the beam is traveling at constant height relative to the table.
6. Insert the Prism 1 Assembly into the beam path such that the beam is a few millimeters from the top of the prism and a few millimeters from the apex of the prism.

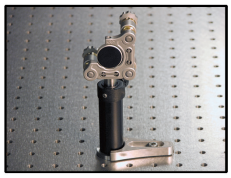
Folding Mirror Assembly

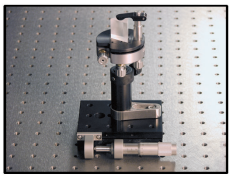
Prism 1 Assembly

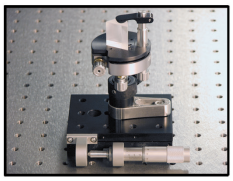
Prism 2 Assembly

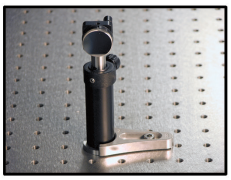
Pickoff Mirror Assembly

Figure 5. Diagrams of the four assemblies

7. Rotate the prism (and mount) such that the beam deviation, δ, from its unaltered path is minimized (see Figure 6). This ensures Brewster angle of incidence on the prism. Move the prism across the beam such that the beam intersects the prism as close to the apex as possible without any observable clipping.

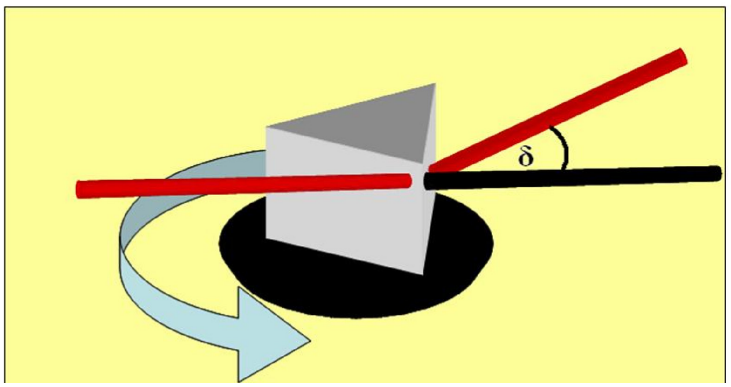

Figure 6. Diagram illustrating angle of minimum deviation

8. Using the tip/tilt adjustment on the prism table, ensure that the beam is traveling at constant height after exiting the prism.
9. Insert the Prism 2 Assembly into the beam path and secure the translation stage to the optical table. Take care that the distance between the apex of Prism 1 and the apex of Prism 2 is at least equal to the value determined in Step 3.
10. Repeat Step 7 for the Prism Assembly 2.
11. Secure the Folding Mirror Assembly after the second prism as shown in Figure 7.

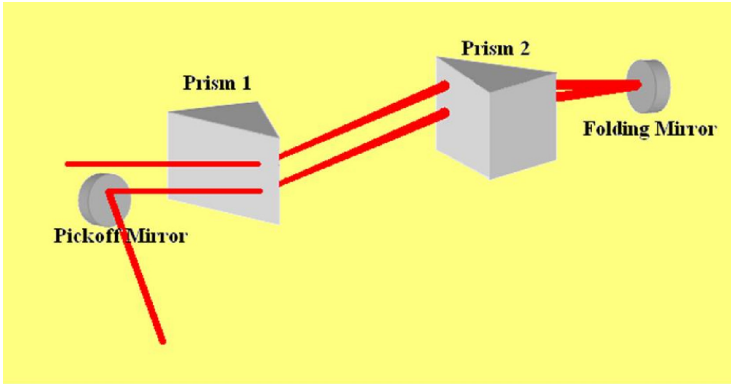

Figure 7. The prism compressor (folded geometry)

12. Send the beam back on itself with a slight vertical displacement of a few degrees depending on the separation between prisms.
13. Install the Pickoff Mirror Assembly just prior to the Prism 1 Assembly. The top of the pickoff mirror should be as close to the incoming beam as possible.

14. Fine tune the tip/tilt adjustments on the Folding Mirror Assembly so that the beam exiting the compressor travels in the same vertical plane as the entering beam and intersects the Pickoff Mirror Assembly without clipping the top of the mirror.

15 Use the Pickoff Mirror to route the beam to an autocorrelator.

16. Using the translation stage at the base of the Prism 2 Assembly, move the prism in and out of the beam in order to minimize the pulse width. If, in the process of minimizing the pulse duration, the beam clips on the edge of the prism, increase the prism separation. If, on the other hand, the beam is coming close to the base of the prism, decrease the separation between prisms. Repeat this step until the pulse duration is minimized.

Experimental Results

1. Compression of Spectra-Physics® Broadband Tsunami® oscillator output using a LakL21 Prism Pair

In this experiment, we compress an output pulse from a Tsunami oscillator configured for broadband operation. The beam directly out of the Tsunami (approximately 2 mm diameter at $1/e^2$) is routed to the Spectra-Physics PulseScout™ autocorrelator and spectrometer using a silver mirror. The results of measurement as read by the PulseScout autocorrelator are shown in Figure 8.

The autocorrelation width is 134 fs at FWHM and the bandwidth around 800 nm is 43 nm, FWHM. This corresponds to pulse duration of 94 fs ($\Delta t_{pulse} = \Delta t_{AC}/1.44$ for a Gaussian pulse). The transform limited pulse width is 22 fs, and from equation (9) we calculate the GDD on the pulse to be 729 fs^2. The GDD is due to the output coupler of the laser and routing optics. Solving equation (12) predicts a prism separation of 38 cm for LakL21 glass and 22 cm for SF10 glass. Experimentally, we found the optimal prism separation for LakL21 glass to be 37.0 cm with the compressed pulse duration of 26 fs (see Figure 9). When using SF10 glass prisms, we found the optimal prism separation to be 22 cm with compressed pulse duration of 32 fs. The experimental distances agree with the calculated distances to within a few percent.

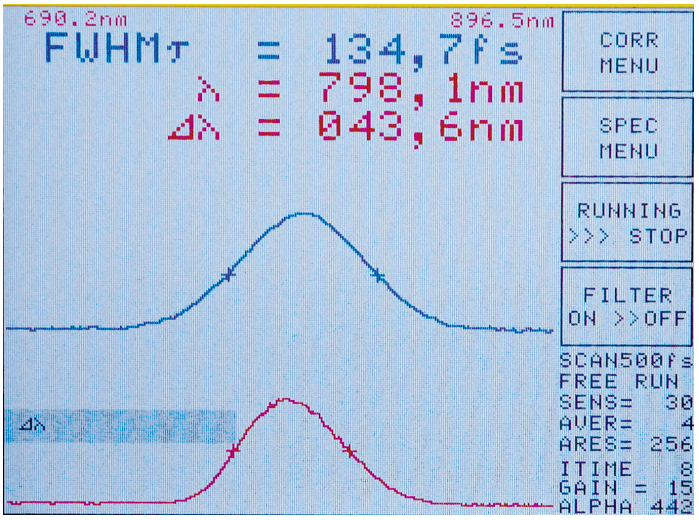

Figure 8. Bandwidth and autocorrelation trace of broadband Tsunami prior to compression

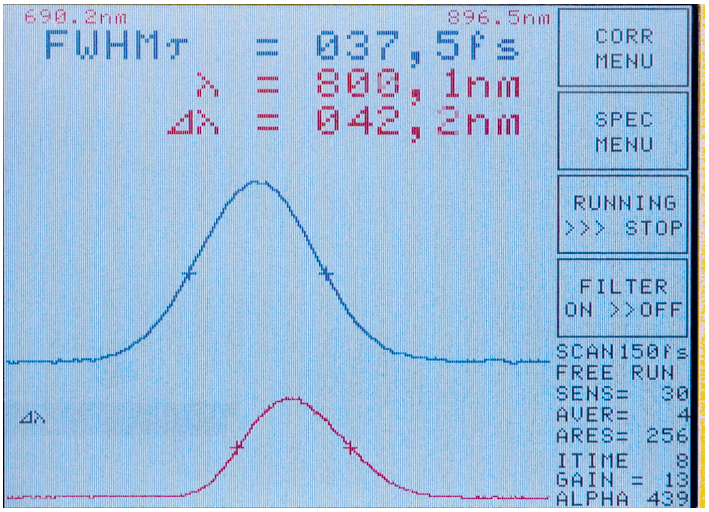

Figure 9. Bandwidth and autocorrelation trace of broadband Tsunami after compression

A prism compressor does not compensate higher order dispersion. SF10 glass has significantly more third order dispersion than LakL21, hence the compressed pulse is 20% longer when using a compressor with SF10 prisms compared to LakL21 prisms. For this reason, SF10 is not recommended for pulses below 50 fs. The PulseScout, used to collect the above autocorrelation traces, can also be used to record the fringe resolved autocorrelation trace as shown in Figure 10.

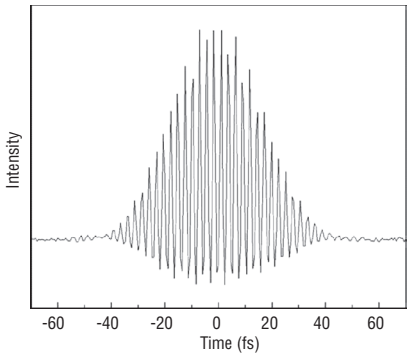

Figure 10. Fringe-resolved autocorrelation trace of compressed output from broadband Tsunami

2. Compression of the Spectra-Physics Tsunami HP using a SF10 Prism Pair

In this experiment, we demonstrate compression of the output pulse of the Tsunami HP oscillator broadened by several optical components. The beam directly out of the Tsunami (approximately 2 mm diameter at $1/e^2$) is routed through a waveplate and polarizer providing variable attenuation of the output power (see Apps. Note 26). After the polarizer, the beam is directed to the PulseScout autocorrelator and spectrometer. We measured the autocorrelation width of 169 fs at FWHM and the bandwidth around 775 nm of 10.5 nm at FWHM. An autocorrelation width of 169 fs corresponds to a pulse duration of 120 fs. Applying the uncertainty principle, we find that the transform limited pulse width is 84 fs, and from equation (9) we find that the GDD on the pulse is 2580 fs^2. The dispersion on the pulse is due to the output coupler, waveplate, calcite polarizer, as well as the routing optics. Taking into account that $GDD_{PRISM} = -GDD_{PULSE}$, equation (12) predicts a prism separation of 30 cm for SF10 glass. Experimentally, we found the optimal prism separation for SF10 glass to be 30 cm with the compressed pulse duration of 85 fs. The experimental distance and pulse duration are in excellent agreement with the calculations. Figure 11 shows that actual prism arrangement used in the experiment.

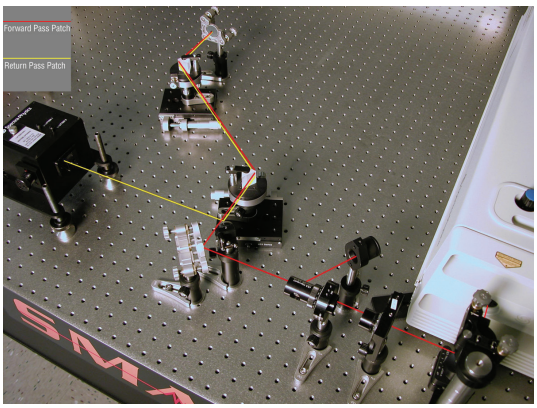

Figure 11. Prism arrangement used to compress the output of Tsunami HP

Conclusions

We demonstrated a simple and cost effective prism compressor for ultrashort laser pulses. The purpose of this compressor is to provide means of controlling dispersion of the femtosecond pulses on a typical experimental set-up that includes oscillators, amplifiers and OPAs. We also provided tables and expressions that will allow users to choose the material of the prisms and determine their optimal separation that will allow the delivery of the shortest pulses to the experiment.

Guide to Appendix 1

Appendix 1 provides a series of tables that can be used to determine the optimum prism separation for the prism compressor described above. Each table is unique for a given wavelength of light and prism material (N-SF10 = N-SF10 glass, N-LakL21 = N-LakL21 glass and FS = Fused Silica). The column header (25 fs – 200 fs) corresponds to the measured pulse width prior to compression. The row header (25 fs - 200 fs [top], bandwidth [bottom]) corresponds to the actual bandwidth (bottom of row) and the transform limited pulse duration (top of row). The matrix elements describe the optimal prism separation (top) and group delay dispersion (bottom) for a combination of pulse width (measured) and bandwidth (measured).

Using the tables is fairly straightforward. For example, in the first experiment described in this note, with the laser operating at 800 nm, the measured pulse width is 94 fs. For a given material, N-LakL21 at 800 nm, we scroll down Column 1 to the pulse width closest to 94 fs (100 fs in this case). Then we scroll across to the column closest to the measured bandwidth (37.5 nm in this case). The corresponding matrix element then gives the approximate prism separation 41 cm and GDD 870 fs^2. The determined prism separation can serve as a good starting point for setting up and optimizing the compressor without solving the equation (12).

Alternatively, if the thickness and dispersive properties of the optical elements in the beam path are known, the GDD can be determined from Table 2 by summing the GVD multiplied by the thickness of each optic. After calculating the GDD, measure the bandwidth of the pulse. For a given material, wavelength, and bandwidth, find the matrix element with the nearest GDD. The correct prism separation is also contained in this matrix element.

Appendix 1 – Tables of Prism Parameters

Fused Silica – 400 nm

	25 fs (9.4 nm)	50 fs (4.7 nm)	75 fs (3.1 nm)	100 fs (2.3 nm)	125 fs (1.9 nm)	150 fs (1.6 nm)	175 fs (1.3 nm)	200 fs (1.2 nm)
25	0	0	0	0	0	0	0	0
50	20 390	0	0	0	0	0	0	0
75	22 640	25 1010	0	0	0	0	0	0
100	24 870	30 1560	32 1790	0	0	0	0	0
125	27 1100	35 2070	41 2710	40 2710	0	0	0	0
150	29 1330	40 2550	48 3510	53 4030	50 3740	0	0	0
175	31 1560	44 3020	56 4280	64 5180	67 5520	60 4880	0	0
200	34 1790	49 3490	63 5020	74 6250	81 7040	82 7160	72 6110	0
200	1789	3492	5015	6247	7038	7156	6111	0

Fused Silica – 800 nm

	25 fs (37.5 nm)	50 fs (18.8 nm)	75 fs (12.5 nm)	100 fs (9.4 nm)	125 fs (7.5 nm)	150 fs (6.3 nm)	175 fs (5.4)	200 fs (4.7 nm)
	25	50	75	100	125	150	175	200
25	0	0	0	0	0	0	0	0
50	49 390	0	0	0	0	0	0	0
75	62 640	77 1010	0	0	0	0	0	0
100	74 870	103 1560	113 1790	0	0	0	0	0
125	85 1100	128 2070	156 2710	155 2710	0	0	0	0
150	97 1330	151 2550	195 3510	218 4030	203 3740	0	0	0
175	108 1560	174 3020	231 4280	272 5180	287 5520	256 4880	0	0
200	120 1790	197 3490	266 5020	323 6250	358 7040	363 7160	313 6110	0

Fused Silica – 550 nm

	25 fs (17.7 nm)	50 fs (8.9 nm)	75 fs (5.9 nm)	100 fs (4.4 nm)	125 fs (3.5 nm)	150 fs (3.0 nm)	175 fs (2.5 nm)	200 fs (2.2 nm)
	25	50	75	100	125	150	175	200
25	0	0	0	0	0	0	0	0
50	37 390	0	0	0	0	0	0	0
75	43 640	50 1010	0	0	0	0	0	0
100	49 870	64 1560	69 1790	0	0	0	0	0
125	55 1100	77 2070	91 2710	91 2710	0	0	0	0
150	62 1330	89 2550	111 3510	123 4030	115 3740	0	0	0
175	68 1560	101 3020	130 4280	151 5180	159 5520	143 4880	0	0
200	73 1790	113 3490	148 5020	177 6250	196 7040	198 7160	172 6110	0

N-LAKL21 – 400 nm

	25 fs (9.4 nm)	50 fs (4.7 nm)	75 fs (3.1 nm)	100 fs (2.3 nm)	125 fs (1.9 nm)	150 fs (1.6 nm)	175 fs (1.3 nm)	200 fs (1.2 nm)
	25	50	75	100	125	150	175	200
25	0	0	0	0	0	0	0	0
50	11 390	0	0	0	0	0	0	0
75	12 640	13 1010	0	0	0	0	0	0
100	13 870	15 1560	16 1790	0	0	0	0	0
125	14 1100	17 2070	19 2710	19 2710	0	0	0	0
150	15 1330	19 2550	22 3510	24 4030	22 3740	0	0	0
175	16 1560	20 3020	25 4280	28 5180	29 5520	26 4880	0	0
200	17 1790	22 3490	27 5020	31 6250	34 7040	34 7160	31 6110	0

N-LAKL21 – 800 nm

	25 fs (37.5 nm)	50 fs (18.8 nm)	75 fs (12.5 nm)	100 fs (9.4 nm)	125 fs (7.5 nm)	150 fs (6.3 nm)	175 fs (5.4)	200 fs (4.7 nm)
	25	50	75	100	125	150	175	200
25	0	0	0	0	0	0	0	0
50	30 390	0	0	0	0	0	0	0
75	35 640	41 1010	0	0	0	0	0	0
100	41 870	53 1560	57 1790	0	0	0	0	0
125	46 1100	64 2070	76 2710	75 2710	0	0	0	0
150	51 1330	74 2550	93 3510	103 4030	96 3740	0	0	0
175	56 1560	84 3020	108 4280	126 5180	133 5520	119 4880	0	0
200	61 1790	94 3490	124 5020	148 6250	164 7160	165 7160	144 6110	0

N-LAKL21 – 550 nm

	25 fs (17.7 nm)	50 fs (8.9 nm)	75 fs (5.9 nm)	100 fs (4.4 nm)	125 fs (3.5 nm)	150 fs (3.0 nm)	175 fs (2.5 nm)	200 fs (2.2 nm)
	25	50	75	100	125	150	175	200
25	0	0	0	0	0	0	0	0
50	21 390	0	0	0	0	0	0	0
75	24 640	26 1010	0	0	0	0	0	0
100	26 870	32 1560	34 1790	0	0	0	0	0
125	29 1100	37 2070	43 2710	42 2710	0	0	0	0
150	31 1330	42 2550	51 3510	55 4030	52 3740	0	0	0
175	34 1560	47 3020	58 4280	66 5180	69 5520	63 4880	0	0
200	36 1790	51 3490	65 5020	77 6250	84 7040	85 7160	75 6110	0

N-SF10 – 400 nm

	25 fs (9.4 nm)	50 fs (4.7 nm)	75 fs (3.1 nm)	100 fs (2.3 nm)	125 fs (1.9 nm)	150 fs (1.6 nm)	175 fs (1.3 nm)	200 fs (1.2 nm)
	25	50	75	100	125	150	175	200
25	0	0	0	0	0	0	0	0
50	5 390	0	0	0	0	0	0	0
75	5 640	5 1010	0	0	0	0	0	0
100	5 870	5 1560	5 1790	0	0	0	0	0
125	5 1100	5 2070	5 2710	5 2710	0	0	0	0
150	5 1330	5 2550	6 3510	6 4030	6 3740	0	0	0
175	5 1560	5 3020	6 4280	6 5180	6 5520	6 4880	0	0
200	5 1790	6 3490	6 5020	7 6250	7 7040	7 7160	6 6110	0

N-SF10 – 800 nm

	25 fs (37.5 nm)	50 fs (18.8 nm)	75 fs (12.5 nm)	100 fs (9.4 nm)	125 fs (7.5 nm)	150 fs (6.3 nm)	175 fs (5.4)	200 fs (4.7 nm)
	25	50	75	100	125	150	175	200
25	0	0	0	0	0	0	0	0
50	19 390	0	0	0	0	0	0	0
75	21 640	21 1010	0	0	0	0	0	0
100	22 870	25 1560	25 1790	0	0	0	0	0
125	24 1100	28 2070	31 2710	30 2710	0	0	0	0
150	25 1330	31 2550	36 3510	38 4030	36 3740	0	0	0
175	27 1560	33 3020	40 4280	45 5180	46 5520	42 4880	0	0
200	28 1790	36 3490	44 5020	51 6250	55 7040	56 7160	49 6110	0

N-SF10 – 550 nm

	25 fs (17.7 nm)	50 fs (8.9 nm)	75 fs (5.9 nm)	100 fs (4.4 nm)	125 fs (3.5 nm)	150 fs (3.0 nm)	175 fs (2.5 nm)	200 fs (2.2 nm)
	25	50	75	100	125	150	175	200
25	0	0	0	0	0	0	0	0
50	10 390	0	0	0	0	0	0	0
75	10 640	10 1010	0	0	0	0	0	0
100	10 870	11 1560	11 1790	0	0	0	0	0
125	11 1100	12 2070	13 2710	13 2710	0	0	0	0
150	11 1330	13 2550	14 3510	15 4030	14 3740	0	0	0
175	12 1560	14 3020	15 4280	17 5180	17 5520	16 4880	0	0
200	12 1790	14 3490	17 5020	19 6250	20 7040	20 7160	18 6110	0

N-BK7 – 400 nm

	25 fs (9.4 nm)	50 fs (4.7 nm)	75 fs (3.1 nm)	100 fs (2.3 nm)	125 fs (1.9 nm)	150 fs (1.6 nm)	175 fs (1.3 nm)	200 fs (1.2 nm)
	25	50	75	100	125	150	175	200
25	0	0	0	0	0	0	0	0
50	15 390	0	0	0	0	0	0	0
75	17 637	19 1008	0	0	0	0	0	0
125	19 873	22 1561	23 1789	0	0	0	0	0
100	20 1104	26 2066	29 2705	29 2705	0	0	0	0
150	22 1333	29 2550	34 3513	38 4032	35 3738	0	0	0
175	23 1561	32 3024	39 4277	45 5179	47 5521	43 4876	0	0
200	25 1789	35 3492	44 5015	52 6247	56 7038	57 7156	50 6111	0

N-BK7 – 800 nm

	25 fs (37.5 nm)	50 fs (18.8 nm)	75 fs (12.5 nm)	100 fs (9.4 nm)	125 fs (7.5 nm)	150 fs (6.3 nm)	175 fs (5.4)	200 fs (4.7 nm)
	25	50	75	100	125	150	175	200
25	0	0	0	0	0	0	0	0
50	42 390	0	0	0	0	0	0	0
75	52 637	63 1008	0	0	0	0	0	0
125	61 873	83 1561	90 1789	0	0	0	0	0
100	70 1104	102 2066	123 2705	122 2705	0	0	0	0
150	79 1333	120 2550	153 3513	170 4032	159 3738	0	0	0
175	88 1561	137 3024	180 4277	211 5179	222 5521	199 4876	0	0
200	97 1789	154 3492	207 5015	250 6247	277 7038	280 7156	242 6111	0

N-BK7 – 550 nm

	25 fs (17.7 nm)	50 fs (8.9 nm)	75 fs (5.9 nm)	100 fs (4.4 nm)	125 fs (3.5 nm)	150 fs (3.0 nm)	175 fs (2.5 nm)	200 fs (2.2 nm)
	25	50	75	100	125	150	175	200
25	0	0	0	0	0	0	0	0
50	30 390	0	0	0	0	0	0	0
75	34 637	39 1008	0	0	0	0	0	0
125	39 873	49 1561	52 1789	0	0	0	0	0
100	43 1104	58 2066	68 2705	67 2705	0	0	0	0
150	47 1333	66 2550	82 3513	90 4032	84 3738	0	0	0
175	51 1561	74 3024	95 4277	110 5179	115 5521	104 4876	0	0
200	55 1789	83 3492	108 5015	128 6247	141 7038	142 7156	124 6111	0

References

1. *J. Diels and W. Rudolf, Ultrashort Laser Pulse Phenomena, Second Edition (Massachusetts, Academic Press, 2006).*
2. *E. Oran Brigham, The Fast Fourier Transform: An Introduction to Its Theory and Application (New Jersey, Prentice Hall, 1973).*
3. *R. Trebino, Frequency-Resolved Optical Gating: The Measurement of Ultrashort Laser Pulse (Massachusetts, Kluwer Academic Publishers, 2002).*
4. *R.L. Fork, O.E. Martinez, and J.P. Gordon, (Opt. Lett. 9, 150 1984).*
5. *R.E. Sheriff, (J. Opt. Soc. Am. B 15, 1224 1998).*

mks | Newport

www.newport.com | sales@newport.com

+1-949-863-3144 | +1-800-222-6440

DS-11065 (03/21)